Path Loss Model for Heterogeneous Environments: A Land Cover Segmentation Approach

Samuel Santos Troina
Technological Development Center
Federal University of Pelotas
Pelotas, Brazil
samuel.troina@gmail.com

Maiquel dos Santos Canabarro
Engineering Center
Federal University of Pelotas
Pelotas, Brazil
canabarrom@gmail.com

Felipe de Souza Marques
Technological Development Center
Federal University of Pelotas
Pelotas, Brazil
felipem@inf.ufpel.edu.br

***Abstract*—Wireless communication technology is already ubiquitous in our lives and can be considered almost essential. We are currently experiencing the so-called economy 4.0, which focuses on using new technologies to develop solutions to societal challenges. In this new revolution, the physical world is becoming increasingly integrated with the digital world, where the majority of new technologies applied in areas such as smart cities, agriculture, industries, healthcare, and logistics, require communication to bridge the gap between the worlds. In this context, wireless communication adoption emerges as the most promising technology. However, significant challenges arise due to factors that primarily influence signal propagation in a given environment. Natural elements or artificial presents in the ambiance interact with the signal in many ways, often resulting in signal attenuation or complete signal blockage. This empirical research focuses on predicting signal loss intensity in heterogeneous land cover. It explores LoRa technology in environments characterized by both obstructed and unobstructed paths. The results demonstrate that adopting the strategy of segmenting the signal path based on terrain coverage is an alternative that brings more precise results in estimating signal loss. This study observed an average error of 2.58 dBm for environments with uniform land cover and 3.49 dBm for mixed coverage when using a predictive model that segments the signal path.**

***Index Terms*—LoRa, Path Loss, Log-Distance, Wireless Sensor Network, Coverage, Internet of Things**

I. Introduction

Economy 4.0 includes many sectors, such as smart cities, agribusiness, industries, healthcare, logistics, and others. One of its key pillars is connectivity, which facilitates the integration and exchange of information among different systems and devices [6].

Wireless networks, especially Low Power Wide Area Networks (LPWAN), have attracted attention from the scientific community due to their ability to perform long-range communication with low power consumption. Among LPWAN technologies, LoRa technology has been significantly highlighted [12]. However, effectively deploying networks in environments with heterogeneous land cover brings challenges. Some characteristics, such as dense vegetation, topography, natural obstacles, and interferences, can significantly impact signal propagation, bringing decreased signal strength and network performance degradation [9].

Deployment of a wireless network requires careful analysis of how signal propagation will happen, taking into account the specific characteristics of the environment. In environments with heterogeneous land cover, it is essential to understand and assess the influence of different terrain conditions. In our case, we will explore LoRa signal propagation. Accurate modeling and characterization of the signal under these conditions can provide valuable insights for network planning, dimensioning, and optimization, ensuring reliable and efficient communication in challenging environments [7].

Traditionally, the process implementation of a new network begins with a site survey, which involves measuring signal strength and quality transmission at predetermined points. However, this process relies on human and financial resources to be carried out, in addition to the precise selection of the analyzed points of interest, which must be accessible and representative.

In this context, path loss models used for characterizing signal propagation behavior offer advantages in analyzing complex environments. Implementing a network can be challenging due to difficulties in accessing the environment, high costs, and the time required for traditional measurement methods. In such situations, using reliable predictive models becomes indispensable [4].

Because of the above, it is evident the need to models that consider, in addition to the particularities of LPWAN technologies, the characteristics of the environments to obtain more accurate and reliable results, contributing to more efficient planning of the positioning of the network nodes and guaranteeing in a way best suited for connectivity.

II. Related work

The signal strength is directly influenced by the characteristics and phenomena present in the ambient where it is propagated. These characteristics are expressed, by a term, in the equation that represents the rate at which the signal power decreases. The signal decrease rate typically ranges between 2 and 6. Rate 2 is commonly used in line-of-sight propagations, while higher rates are applied in locations where there are more attenuation factors [8].

In the literature, there are a lot of studies about LoRa signal propagation. [13] evaluated the impact of the device's antenna

height on path loss, and he proposed a modification in the Log-Normal model. This modification added another variable in the model equation, relating signal loss with the antenna height.

Other studies compare the performance between values collected with the predicted by models. [18] made a comparison between Log-Distance and Okumura-Hata models. It found that the Log-Distance model performs better.

[17] presents a model where the transmission distance is divided into two classes: those that are in line-of-sight and those that occur with total or partial obstruction. The identification of the segments occurs through the analysis of the data obtained with a Digital Surface Model (DSM). The path loss of the line-of-sight group is determined using the Free Space model, while segments with obstruction are determined and compared with the Weissberger, ITU-R, COST235, FITU-R, and lateral ITU-R models.

[14]–[16] used AI to classify the land cover of a signal path, for example, in vegetation, open fields, roads, water, and buildings, and segmented it by land coverage classification. In [14], the land cover is classified into two groups, with line-of-sight (LOS) and without line-of-sight (NLOS). This segmentation will determine which variation of the Okumura-Hata model to utilize.

III. LoRa technology

LoRa is an acronym for Long-Range, it is an LPWAN communication technology owned by the company Semtech. Its physical layer employs the Chirp Spread Spectrum Modulation (CSS) modulation technique.

LoRa modulation is composed of five parameters: carrier frequency (CF), bandwidth (BW), transmit power (TP), spreading factor (SF), and coding rate (CR). The different combinations used in the transmission parameters make it possible, for example, to increase the transmission rate, extend the transmission range, increase the robustness to interference, and also reduce consumption energy consumption, among others.

The maximum LoRa packet size differs by region due to local regulations. In Brazil, the frequency bands commonly employed are 902-907.5 MHz and 915-928 MHz. It also established that the maximum time on air for packet transmission is 400 milliseconds. [11].

The technical report [1] presents equations for calculating the Time of Arrival (TOA) of a packet in the air. Below, Table I presents the time on air for the bandwidth 125 kHz when spreading factors 7 to 10 are employed. The SF 11 and 12 cannot be applied because they have a time on air greater than 400 ms.

TABLE I
Maximum payload length, TOA, duty cycle, and sensitivity about BW and SF using CR 4/5

BW	SF	Payload	TOA	Duty Cicle	Sensitivity
125 kHz	7	255	399,62	0:00:40	-124 dBm
	8	138	399,87	0:00:40	-127 dBm
	9	66	390,14	0:00:39	-130 dBm
	10	24	370,69	0:00:37	-133 dBm

IV. Path Loss models

A. Free Space

The Free Space propagation model, also known as the *Friis* model, is the basis for understanding other complex models [2]. It is a theoretical/fundamental model because it considers that there are no obstacles in the environment that could interfere with the transmitted signal, that is, there is no interference of the signal, either by obstruction or reflection. Furthemore, it assumes that the transmitter is always in line of sight (LOS) with the receiver. However, these characteristics are not suitable for most situations where WSNs are applied [5], [9].

$$FSPL(dBm) = 20\log_{10}(d) + 20\log_{10}(f) - 147.55 \quad (1)$$

where d is the distance separating the transmitter from the receiver in meters and f is the frequency in Hertz.

B. Log-Distance

Is an extension of the *Free Space* model. The difference between them is that it allows predicting the *Path Loss* for different kinds of environments, including those with line-of-sight obstructions. In contrast, the *Free Space* model is used only in scenarios where a direct line-of-sight exists between the transmitter and receiver.

According to [3], the average reception power of the signal decreases logarithmically as the distance between transmitter and receiver increases, with the *Log-Distance* model defined by the equation 2:

$$PL(d) = PL(d_0) + 10n\log_{10}\left(\frac{d}{d_0}\right), d \geq d_0 \quad (2)$$

where n is the path loss exponent, which indicates the rate of the signal intensity decrease with increasing distance. d_0 value corresponds to a reference distance used to determine $PL(d_0)$, which is the path loss at that specific distance. Generally, $PL(d_0)$ is calculated by the *Free Space* model or by measurements taken at the reference distance. It is important to note that the reference distance should be outside the near-field region (equal to or greater than the *Fraunhofer* distance). This precaution is essential to ensure that the measurements of signal loss remain unaffected by near-field effects. Lastly, d denotes the distance between the transmitter and the receiver.

C. SateLoc

Based on the Log-Distance, [16] proposes an interactive approach that segments the signal path based on changes in terrain coverage. The proposed model consists of the equation:

$$PL(d_k) = PL(d_0) + \sum_{k=i}^{k}\left(10n_{(d_{k-1},d_k)}\log_{10}\frac{d_k}{d_{k-1}}\right) \quad (3)$$

where:

- d_1,d_2...d_k corresponds to the distances between the link segments and the gateway;
- $n_{(d_{k-1},d_k)}$ path loss exponent by land cover;

V. Devices and Methods

To measure the propagation of the LoRa signal, we developed a communication device prototype that uses a LoRaMESH communication module, which integrates the SX1272 transceiver, which is commercialized by the Radioenge company. Additionally, the prototype includes an ESP8266-01 module, which supports Wi-Fi networks. This allows us to control the prototype device using a smartphone via a wireless network.

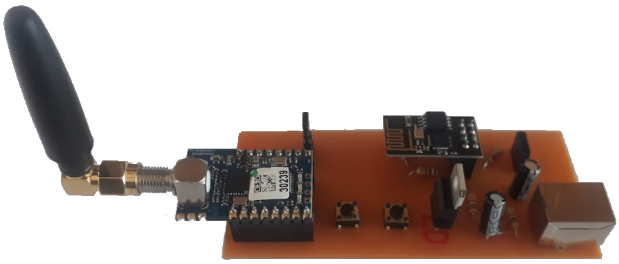

Fig. 1. LoRaMESH and ESP8266-01 Module integration circuit.

All tests made respected local law, as shown in Table I. However, only the parameterizations defined by the LoRaWAN standard were adopted, corresponding to the AU915-928 plans, observing only those corresponding to the direction of communication towards the gateway.

For each environment under investigation, we collected 20 samples of received signal strength (RSSI) at various distances. The samples were taken at 5-second intervals, employing the transmission parameters specified in Table I to ensure a more precise average of signal intensity.

During the data collection, the devices were positioned at a height of 1.5 meters above the ground, equipped with 3 dBi antennas, and were in a stationary position during the tests to get better stability in the results. This decision was based on a study conducted by [10], which indicated that mobile transmissions can be adversely impacted by the Doppler effect.

The impact of transmission power on received signal strength was also examined. During the conducted tests, the power was adjusted in the range of 11 dBm to 20 dBm, with increments of 3 dBm. This specific range was chosen because each 3 dBm reduction in transmission power results in a halving of power in Watts.

Finally, in order to evaluate the performance of the path loss models, we employed two metrics: Mean Absolute Error (MAE) and Mean Squared Error (MSE).

VI. Experiments

A. Transceiver Calibration

To accurately measure the signal loss intensity, was carried an analysis of the real transmission power of the *LoRaMESH* module. Because we didn't have access to a spectrum analyzer with the necessary accuracy, we conducted tests using a pair of *LoRaMESH* modules interconnecting them directly by a cable. These tests consisted of collecting 200 samples of RSSI values, using different transmission powers and spreading factors.

Figure 2 shows the setup used, in which the transceiver module is always connected to a power attenuator of 30 dB since the maximum power supported by the module is of 10 dBm.

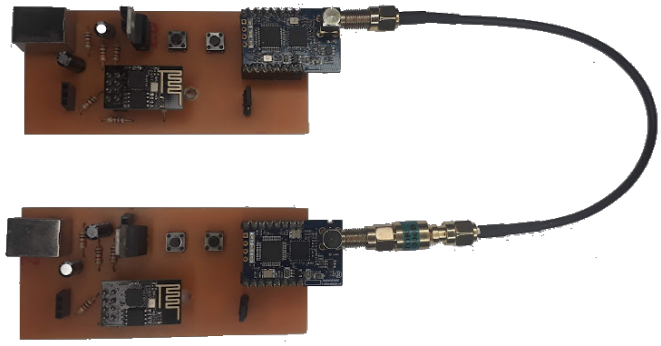

Fig. 2. Pair of *LoRaMESH* modules interconnected directly by a cable with a 30 dBm attenuator.

It is important to notice that the obtained results in the analysis have considered approximate values due to the limitations of the equipment in terms of precision. However, these measurements provided a closer estimation of the actual transmit power to the defined transmit settings.

The evaluation of the transmission power of the LoRaMESH module revealed that even though it was parameterized for transmission with the power of 20 dBm, it didn't exceed 14 dBm. We observed that the spreading factor influenced the transmission power, as the module's transmission power changed as the parameterized spreading factor.

Table II presents the correlations established and used to reference the used transmission power.

TABLE II
Correlation between the parameterized powers and those measured

PW	SF 10	SF 9	SF 8	SF 7
20 dBm	7.50 dBm	8.15 dBm	8.69 dBm	13.64 dBm
17 dBm	6.64 dBm	7.48 dBm	8.01 dBm	12.77 dBm
14 dBm	4.87 dBm	5.08 dBm	5.91 dBm	9.50 dBm
11 dBm	2.42 dBm	2.87 dBm	3.58 dBm	7.33 dBm

To verify the accuracy of the attenuator's attenuation, we used the signal generator of the TinySA spectrum analyzer. The test involved the measuring of the signal power with and without the attenuator to assess the reduction in signal strength. The results confirmed that the signal power was accurately attenuated by -30 db as expected.

B. Reference campaign

This campaign aimed to ensure greater confiability of the collected data in the measurement campaigns, analyzing the

behavior of the signal about the measured values. This analysis evaluated the collected data aligned with expectations for line-of-sight (LOS) measurements, using the Free Space model as a reference.

The tests for this campaign were at Cassino Beach, located in the Rio Grande city, in Rio Grande do Sul, Brazil. This location was chosen due to its expansive, flat, and uninterrupted sandy area, providing an ideal line-of-sight condition for the tests. Conducting the tests in this environment facilitated a more precise evaluation of signal attenuation, devoid of any interference caused by obstacles. As a result, it closely reflected the signal attenuation in an obstruction-free environment.

In this campaign, data measurements followed a predefined methodology, with reference distances ranging from 1 to 5 meters between the devices.

The table in Figure 1 provides the average values of a hundred RSSI samples at a distance of 1 meter, considering different transmission power and spreading factor configurations. The path loss (PL) was calculated using equation 4, where the average RSSI value was used in the term corresponding to the received power.

$$PL = (P_{t(dBm)} + G_{t(dBi)}) - (G_{r(dBi)} + P_{r(dBm)}) \quad (4)$$

where $P_{t(dBm)}$ is the transmission power, $G_{t(dBi)}$ and $G_{r(dBi)}$ refer to the transmitter and receiver antenna gain, and P_r is the strength of signal received by the receiver.

1 meter (BW 125khz)													
FSPL (dBm)	Pt	Spreading Factor											
		RSSI (dBm)				IRL = RSSI - 3dBi				PL (dBm) = EIRP - IRL			
		10	9	8	7	10	9	8	7	10	9	8	7
31.56	20	-21.41	-20.74	-20.29	-15.42	-24.41	-23.74	-23.29	-18.42	34.91	34.89	34.98	35.06
	17	-22.78	-22.14	-21.59	-16.64	-25.78	-25.14	-24.59	-19.64	35.42	35.62	35.60	35.41
	14	-26.92	-26.88	-26.33	-20.56	-29.92	-29.88	-29.33	-23.56	37.79	37.96	38.24	36.06
	11	-26.75	-26.43	-25.57	-21.82	-29.75	-29.43	-28.57	-24.82	35.17	35.30	35.15	35.15

Fig. 3. Result of collecting the referential PL values at 1 meter away.

Analyzing the results obtained at a distance of 1 meter, it is evident that the signal intensity losses exceed the predicted value of 31.56 dBm by the Free Space model. The closest value obtained was 36.42 dBm when using the transmission power of 15 dBm combined with a spreading factor of 7. However, even though the value is close, there is a significant difference compared to the theoretical model, being approximately 13% larger.

Therefore, inorder to compensate the difference identified between the values measured and those expected for a LOS environment, a correction factor (FC) was determined, which corresponds to the difference between the path loss obtained in the collection at 1 meter and the path loss calculated by the *Free Space* model, using the equation:

$$FC = PL(Measured) - PL(Free\ Space) \quad (5)$$

Figure 4 shows the correction factors that must be added to the measured RSSI values to decrease the difference, according to parameterized power and spreading factor.

1 meter (BW 125khz)									
FSPL (dBm)	Pt	Spreading Factor							
		PL (dBm) = EIRP - IRL				Correction Factor			
		10	9	8	7	10	9	8	7
31.56	20	34.91	34.89	34.98	35.06	3.35	3.34	3.42	3.50
	17	35.42	35.62	35.60	35.41	3.86	4.07	4.05	3.85
	14	37.79	37.96	38.24	36.06	6.23	6.40	6.68	4.50
	11	35.17	35.30	35.15	35.15	3.61	3.74	3.60	3.59

Fig. 4. Calculated correction factors.

C. Evaluation Campaign

In this campaign, the objective was to analyze the influence of different land covers on signal propagation, with a specific focus on the impact of vegetation. The study area chosen for this analysis was the "Vila Assumpção" neighborhood in Pelotas, Rio Grande do Sul, Brazil. The campaign investigated three distinct scenarios based on the land cover present in each area:

1) Open field: area covered by low and sparse vegetation;
2) Forest: area with dense tree cover;
3) Mixed: an area characterized by a mixture of low and sparse vegetation with another dense tree cover.

Figure 5 displays the two types of land cover found in the area. The first image illustrates the open field land cover, while the second image represents the forest cover.

(a) Open field (b) Forest

Fig. 5. Types of land cover presents in the environment.

The satellite view of the environment, depicted in Figure 6, highlights the test locations and the placement of the gateway and the end devices. Table III provides a detailed overview of the analyzed point combinations and their respective distances.

D. Evaluation of path loss models

The performance evaluation of the models enabled the identification of their accuracy and determination of the model that yields better results when applied to long-distance links with variations in land coverage.

One notable feature of the evaluated models, excluding the Free Space model, is the presence of a power decay exponent (n). This exponent plays a crucial role in determining the rate at which signal strength decreases with distance. Accurate determination of the n value is essential for improving the precision of the models.

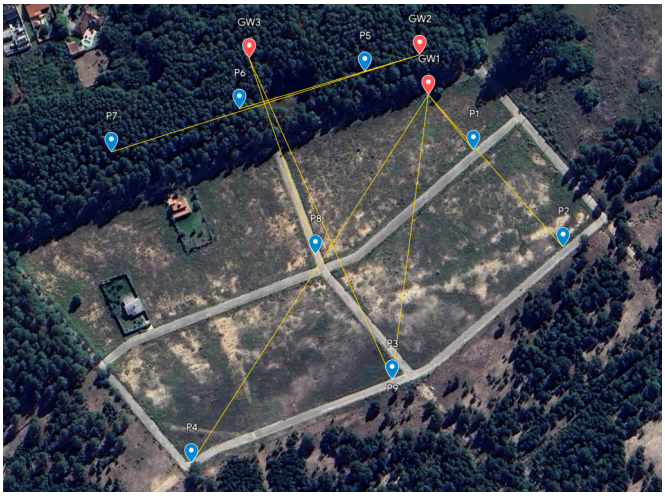

Fig. 6. Placement of the gateway and end devices.

TABLE III
LINKS EVALUATED IN THE 2ND DATA COLLECTION CAMPAIGN AS ILLUSTRATED IN FIGURE 6

Links		Distance	Land Cover
Gateway	End Device		
GW1	P1	65 m	Open field
GW1	P2	184 m	Open field
GW1	P3	252 m	Open field
GW1	P4	389 m	Open field
GW2	P5	50 m	Forest
GW2	P6	170 m	Forest
GW2	P7	288 m	Forest
GW3	P8	185 m	Mixed
GW3	P9	314 m	Mixed

To determine the optimal value of n, we employed the curve fitting technique using the least squares method. In order to determine the most suitable value of n for each land cover under investigation, we utilized the *SciPy* library (https://scipy.org/). Table IV presents the calculated values of n based on the values measured in the campaigns, segmented by type of coverage. The dataset and the notebook are available in the repository [1], containing all the analyzes performed.

TABLE IV
SAMPLES OF $PL(d0)$, $d0$ AND n BY LAND COVER AND POWER FOR THE SF 10 AND 7

Open field		
PW	**SF 10**	**SF 7**
20	20.52, 2.07, 2.67	15.22, 1.99, 3.01
17	20.92, 2.07, 2.62	16.86, 2.42, 3.08
14	19.39, 1.99, 2.60	16.45, 2.18, 2.95
11	18.95, 1.83, 2.71	20.48, 2.84, 2.99
Forest		
PW	**SF 10**	**SF 7**
20	10.20, 4.19, 4.31	9.02, 4.62, 4.67
17	13.37, 4.76, 4.26	3.18, 3.59, 4.78
14	9.27, 4.38, 4.31	0.79, 3.92, 4.93
11	13.37, 4.73, 4.32	7.81, 4.34, 4.74

[1]https://github.com/samuel-troina/doutorado/

The charts displayed in Figure 7 demonstrates the relationship between the path loss exponent and the spreading factor. Higher spreading factors are associated with a lower signal decay rate in comparison to lower spreading factors. This disparity emphasizes the importance of considering the value of n concerning the specific set of LoRa parameters used.

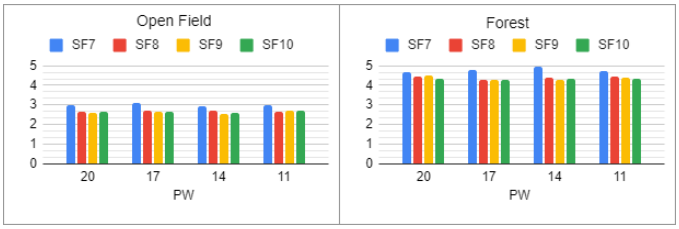

Fig. 7. Graph of path loss exponents by coverage

The models were evaluated using specific reference values for each type of land coverage and the parameterization of the LoRa transceiver. These evaluations were conducted separately, initially focusing on links with homogeneous coverage and subsequently considering links with mixed land coverage. Table V presents the segmented links with different land coverage, indicating the associated distances for each land coverage type.

TABLE V
LINKS WITH MIXED COVERAGE EVALUATED AS SHOWN IN FIGURE 6

Links			Land cover distance		
ID	**Gateway**	**ED**	**Total**	**Open field**	**Forest**
E1	GW3	P8	185 m	110 m	75 m
E2	GW3	P9	314 m	239 m	75 m

Table VI presents the performance evaluation results of the Free Space, Log-Distance, and SateLoc models for links with single-type coverage.

TABLE VI
PERFORMANCE EVALUATION OF FREE SPACE, LOG-DISTANCE, AND SATELOC MODELS IN LINKS WITH SINGLE-TYPE COVERAGE

	MAE	**MAPE**	**MSE**	**RMSE**
FSPL	5.72	0.11	42.13	6.49
Log-Distance	2.00	0.04	6.67	2.58
SateLoc	2.00	0.04	6.67	2.58

Based on the links presented in Table V, which traverse different land coverages, Table VII demonstrates the performance of the models.

TABLE VII
PERFORMANCE EVALUATION OF FREE SPACE AND SATELOC MODELS IN LINKS THAT TRAVERSE DIFFERENT LAND COVERS

	MAE	**MAPE**	**MSE**	**RMSE**
FSPL	2.77	0.03	10.14	3.18
SateLoc	2.99	0.04	12.19	3.49

VII. Conclusions

The tests conducted in this study demonstrated that segmenting the signal path based on terrain coverage leads to more accurate estimations of path loss. Additionally, the SateLoc model has demonstrated its superior predictive performance for path loss in heterogeneous land cover scenarios when utilizing LoRa technology.

The obtained results allowed the evaluation performance of models, demonstrating the effectiveness of the SateLoc model, which outperformed the other evaluated models. Specifically, the SateLoc model exhibited an average error of 3.49 dBm for links traversing different land coverage types.

While the Free Space Path Loss (FSPL) model has demonstrated good performance too, it is important to acknowledge that its accuracy is often compromised in cluttered environments.

Another factor contributing to the increased precision in the obtained results was the adjustment made through the utilization of the correction factor, along with the incorporation of path loss exponents for each group of transmission parameters.

These conclusions highlight the importance of considering land coverage characteristics and using adequate models to estimate path loss in LPWAN networks. This information is essential for planning and optimizing network coverage, ensuring better performance in different environments.

These conclusions are derived from the experiments conducted in this study, highlighting the need for further research in other scenarios and conditions to validate and expand upon these findings.

References

[1] SEMTECH, SX1272 Datasheet.

[2] H. Friis, "A Note on a Simple Transmission Formula," Proceedings of the IRE, vol. 34, pp. 254–256, May 1946.

[3] T. Rappaport, Wireless Communications: Principles and Practice, 2002.

[4] A. Konak, "A kriging approach to predicting coverage in wireless networks," International Journal of Mobile Network Design and Innovation, vol. 3, pp. 65–71, January 2009.

[5] C. Phillips, D. Sicker and D. Grunwald, "A Survey of Wireless Path Loss Prediction and Coverage Mapping Methods," IEEE Communications Surveys & Tutorials, vol. 15, pp. 255–270, March 2013.

[6] A. Rehman, A. Abbasi, N. Islam and Z. Shaikh, "A review of wireless sensors and networks' applications in agriculture," Computer Standards & Interfaces, vol. 36, pp. 236–270, February 2014.

[7] S. Mortazavi, M. Salehe and M. MacGregor, "Maximum WSN coverage in environments of heterogeneous path loss," International Journal of Sensor Networks, vol. 16, pp. 185–198, January 2015.

[8] N. Sirdeshpande and V. Udupi, "Radio range mapping in Wireless Sensor Networks," International Conference on Advances in Human Machine Interaction (HMI), April 2016.

[9] S. Kurt and B. Tavli, "Path-Loss Modeling for Wireless Sensor Networks: A review of models and comparative evaluations," IEEE Antennas and Propagation Magazine, vol. 59, pp. 18–37, February 2017.

[10] J. Petäjäjärvi, K. Mikhaylov, M. Pettissalo, J. Janhunen and J. Iinatti, "Performance of a low-power wide-area network based on LoRa technology: Doppler robustness, scalability, and coverage," International Journal of Distributed Sensor Networks, vol. 13, pp. 255–270, March 2017.

[11] Anatel, Ato nº 14448, de 04 de Dezembro de 2017.

[12] K. Mekki, E. Bajic, F. Chaxel and F. Meyer, "A comparative study of LPWAN technologies for large-scale IoT deployment," ICT Express, vol. 5, pp. 1–7, March 2019.

[13] R. El Chall, S. Lahoud and M. El Helou, "LoRaWAN Network: Radio Propagation Models and Performance Evaluation in Various Environments in Lebanon," IEEE Internet of Things Journal, vol. 6, pp. 2366–2378, April 2019.

[14] S. Demetri, M. Zúñiga, G. P. Picco, F. Kuipers, L. Bruzzone and T. Telkamp, "Automated Estimation of Link Quality for LoRa: A Remote Sensing Approach," 18th ACM/IEEE International Conference on Information Processing in Sensor Networks (IPSN), pp. 145–156, April 2019.

[15] L. Liu, Y. Yao, Z. Cao and M. Zhang, "DeepLoRa: Learning Accurate Path Loss Model for Long Distance Links in LPWAN," IEEE Conference on Computer Communications, May 2021.

[16] Y. Lin, W. Dong, Y. Gao and T. Gu, "SateLoc: A Virtual Fingerprinting Approach to Outdoor LoRa Localization Using Satellite Images," ACM Transactions on Sensor Networks, vol. 17, pp. 1–28, July 2021.

[17] B. Myagmardulam et al., "Path Loss Prediction Model Development in a Mountainous Forest Environment," IEEE Open Journal of the Communications Society, vol. 2, pp. 2494–2501, October 2021.

[18] I. d. S. Batalha et al., "Large-Scale Modeling and Analysis of Uplink and Downlink Channels for LoRa Technology in Suburban Environments," IEEE Internet of Things Journal, vol. 9, pp. 24477–24491, December 2022.